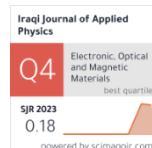


Muthana H Al-Saidi ^{1,2}

¹ Electrical Department,
Faculty of Engineering,
University of Kufa,
Najaf, IRAQ

² Nanotechnology and Advanced
Material Research Unit,
Faculty of Engineering,
University of Kufa,
Najaf, IRAQ

* Corresponding author:
muthanah.alali@uokufa.edu.iq



Synthesis of Silver Nanoparticles via Pulsed Laser Ablation in Liquid and Their Antibacterial Evaluation

Silver nanoparticles were prepared by pulsed laser ablation. Their physical and chemical properties were studied utilizing various techniques, including structural and morphological analysis. The silver nanoparticles exhibited a distinct absorption peak at approximately 425 nm in UV-visible spectroscopy, confirming particle formation. The optical band gap was estimated to be approximately 2.3 eV, indicating distinct electronic properties. X-ray diffraction (XRD) analysis revealed a crystalline phase of the silver nanoparticles. Field-emission scanning electron microscopy (FE-SEM) images revealed spherical particles with an average size ranging from 10 to 50 nm. Fourier-transform infrared (FTIR) spectroscopy revealed changes in the chemical bonds and surface functionalities of the particles. The particles demonstrated antimicrobial activity against *Escherichia coli* (Gram-negative) and *Staphylococcus aureus* (Gram-positive), with higher efficacy against Gram-negative bacteria.

Keywords: Silver nanoparticles; Pulsed-laser ablation; Structural properties; Antibacterial activity
Received: 7 May 2025; Revised: 15 July 2025; Accepted: 22 July 2025; Published: 1 January 2026

1. Introduction

Nanotechnology is among the most advanced and widespread fields of study in today's world since it has a wide range of applications in various fields Such as medicine, pharmacy, engineering, environment and other sciences [1]. Nanomaterials possess the typical small size range of 10 to 100 nanometers, which leads to their characteristic physical and chemical properties [2]. They are the right materials for a wide range of applications including the fabrication of high-performance electronics, cosmetic improvement, and designing efficient delivery systems for drugs and chemicals [3]. Nanotechnology is a useful technique in the fabrication of innovative solutions with improved performance and efficiency in various industries [4].

Nanoparticles may be synthesized by a different way, physics, chemistry or biology processes that can be divided into two general categories: "bottom-up" and "top-down" [5]. In the "bottom-up" process, nanoparticles are built using small atoms and molecules, while in the "top-down" process, large materials are broken down to small particles step by step until nanoparticles are achieved [6]. Pulsed laser ablation in liquids (PLAL) is a prominent example of the "top-down" technique, in which a solid target is irradiated with laser pulses to ablation of particles from the target surface and formation of nanoparticles [7]. This method has several advantages, such as producing pure nanoparticles, environmentally friendly method

because it is possible not to use chemicals and precise control of particle size by adjusting the parameters of the laser and the surrounding medium [8].

PLAL is a convenient method for producing nanoparticles, such as silver nanoparticles, which have important applications in medicine and biology [9]. In PLAL, laser pulses are directed at the surface of a solid material immersed in a liquid (such as water or ethanol), resulting in the ablation of the material into nanoparticles [10]. The synthesis of silver nanoparticles by PLAL is superior to some conventional methods [11]. First, the process allows the synthesis of nanoparticles in their pure form without the presence of any other chemical or reducing agent, thus reducing environmental risks and pollution [12]. Second, the size of the resulting particle can be controlled by varying the laser parameters, i.e., power and pulse width, and the surrounding liquid medium [13]. This control enables the physical and chemical properties of the nanoparticles to be tailored to a specific application. The synthesis of silver nanoparticles via this technique has shown high efficacy in therapeutic applications [14]. Nanosilver has antibacterial, antifungal, and antiviral properties, making it an excellent choice for treating infectious diseases [15-17]. Studies have confirmed the high effectiveness of nanosilver in inhibiting microbial growth, providing treatments that are superior to

traditional methods, which cause toxicity and side effects [18-20].

The novelty of this work is founded on the use of PLAL technology as a chemical-free and clean process to synthesize silver nanoparticles with monodisperse shape and size between 10 to 50 nm without any surfactants or reducing agent. The method allows for the formation of highly pure nanoparticles directly dispersed in water. The particles that were synthesized also showed greater antibacterial activity, particularly against *E. coli*, with inhibition zones of 21 mm, which was superior to that of other conventional nanomaterials. These results justify the effectiveness of silver nanoparticles synthesized under these conditions in biomedical applications.

2. Experimental Part

A piece of 99.9% pure silver metal purchased locally was used as showed in Fig. (1). High-purity water with a resistivity of approximately 17.6 MΩ cm at room temperature (25°C) was used as the liquid medium for this technique. The water was obtained using a Milli-Q purification system to ensure minimal impurities in the sample, no contamination, and the formation of stable nanoparticles.



Fig. (1) A silver item and the percentage purity indicated on it

A silver nanoparticles colloidal solution was prepared via the technique of PLAL. Pure metal silver (99.9%) was selected as a target material for the experiment, where the silver sample was placed at the bottom of a glass vessel inside distilled water. A 4 mL volume of water, which provided a height of 9 mm above the silver substrate, was utilized to allow optimum interaction of the laser with the target.

The Nd:YAG laser is operated with a wavelength of 1064 nm, a pulse energy of 900 mJ, and a repetition rate of 5 Hz. The laser beam was focused onto the Ag metal target by a convex lens ($f = 10$ cm) to achieve a spot diameter of about 1 mm, with a total of 300 pulses. These conditions contributed to the removal of material particles from the surface of the sample and their

subsequent precipitation or suspension in the water to form nanoparticles. The laser fluence used in sample preparation was calculated by the following equation:

$$Fluence \left(\frac{J}{cm^2} \right) = \frac{E}{\pi r^2} \quad (1)$$

After calculating the laser beam fluence, it was found to be approximately 114.6 J/cm², which is within the typical range for effective PLAL. This factor is very important in determining the efficiency of this method, the size of the generated nanoparticles, and the concentration in the sample, and was therefore taken into account before conducting this experiment. After completing the sample preparation process, in order to protect it from external influences such as light and temperature, it was placed in an opaque glass container in a dark box at approximately room temperature (~25°C). It was left for several days and then examined again. It was found that the colloidal solution was not affected and remained stable, with no clumping or sedimentation observed, noting that no stabilizers were added to the sample.

3. Result and Discussion

The FTIR spectrum in Fig. (2) shows a characteristic band at 437 cm⁻¹ attributed to the stretching vibrations of the Ag–O bond, indicating the formation of bonds between silver and oxygen. This indicates surface oxidation or interaction between the silver nanoparticles and oxygen molecules in the surrounding medium during the laser pulse process. This interaction contributes to the stabilization of the surface structure of the particles and the formation of oxidized species on their surfaces. In addition, the FTIR spectrum of the nanosilver showed a broad absorption peak around 3400 cm⁻¹, attributed to the stretching vibrations of the O–H bond, which could be attributed to water adsorption or the presence of hydroxyl groups on the surface resulting from exposure to air.

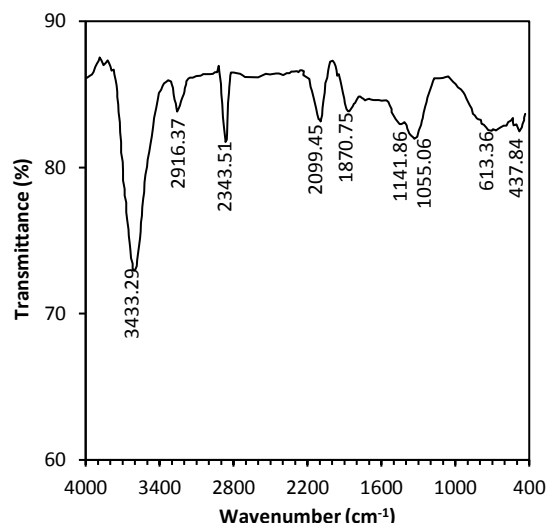


Fig. (2) FTIR spectrum of Ag NPs

The absence of peaks in the spectral range 1630–1650 cm⁻¹ indicates the absence of carbonyl groups (C=O), indicating the absence of significant organic contamination. The weak peaks in the range 1000–1100 cm⁻¹ may be due to C–O vibrations, possibly resulting from simple contact with glass or plastic storage containers. These surface functional groups are due to interactions with the surrounding environment and not to the silver itself.

Figure (3) shows the UV-visible absorption spectra of silver colloids, with a pronounced absorption peak at 425 nm. This peak is characteristic of the localized surface plasmon resonance (LSPR) effect, which occurs as a result of the vibration of free electrons on the surface of nanoparticles when they interact with light. The 425 nm wavelength is an indicator of the particle size and shape of silver nanoparticles and is generally associated with small (20-100nm) and spherical (oval) particles. The maximum absorption is an indicator of good stability and distribution in the nanoparticle solution. This absorption can be utilized in optics application, e.g., sensors, or chemical analysis, whereby the change in the absorption spectrum is tracked in order to sense interactions with other molecules. This characteristic also renders silver nanoparticles amenable in phototherapy methods and nanophotonic devices like optical sensors.

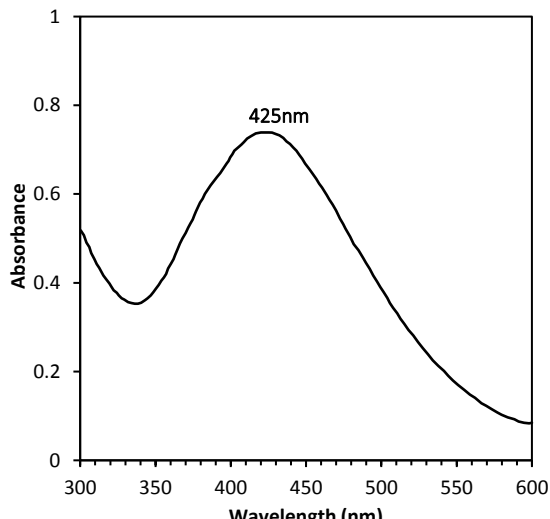


Fig. (3) UV-visible spectrum of Ag NPs

Figure (4), from UV-visible spectroscopy measurements, shows light absorption at 2.3 eV for silver nanoparticles prepared through pulsed laser ablation and represents a very sharp change in the optical property of the material compared to microscopic or macro-sized silver particles. Silver nanoparticles possess distinctive optical properties due to the effect of an increase in surface area relative to volume resulting from the nanoscale size of the material, in addition to the surface plasmon resonance

(SPR) phenomenon. This behavior can be summarized as follows:

- 1- Surface plasmon resonance (SPR): When particles are reduced to a nanoscale size, the conductive electrons oscillate collectively on the surface of the nanoparticles, resembling a single object, in concert with the incident radiation. This results in a strong size-dependent peak in the absorption spectrum, appearing in the visible range.
- 2- Quantum size effects (limited): When particles are reduced to only a few nanometers in size, minor quantum effects may occur that alter the density of electronic states. This effect in Ag nanoparticles is an improvement of the material's optical and electronic properties. It is not the creation of an actual band gap like in the case of semiconductors. These properties of Ag nanoparticles are significantly enhanced by this quantum effect, which makes them special and appropriate for numerous engineering and medical applications. Silver nanoparticles that are excited in the light form reactive oxygen species (ROS), which destroy and kill microbes' cell membranes.

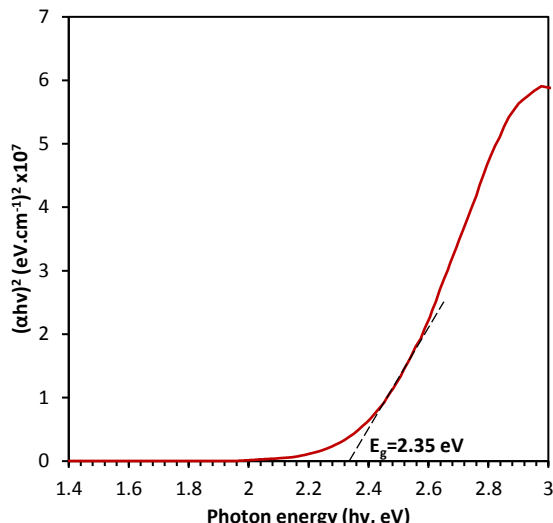


Fig. (4) Determination of the energy gap of Ag NPs

The X-ray diffraction was used to analyze the crystal structure of the silver nanoparticles prepared by pulsed laser technique. The XRD spectrum showed clear peaks at 2θ corresponding to the (111), (200), and (220) crystal planes, confirming that the crystal structure is face-centered cubic (f.c.c.).

The crystallite size was calculated from Scherrer's equation:

$$D = \frac{K\lambda}{\beta \cos \theta} \quad (2)$$

where D is the crystallite size (in nm), which represents the approximate crystal size in the direction perpendicular to the crystal plane, K is Scherrer's constant, a value depending on the shape of the crystal (usually taken to be 0.9), λ is the wavelength of the X-

rays used (usually $\text{Cu-K}\alpha = 1.5406\text{\AA}$), β is the full-width at half maximum (FWHM) of the peak (in rad), and θ is Bragg's angle (in degrees).

Using XRD data and calculating the crystallite size using the Scherrer's equation, it was found to be in the range of 10-50 nm, which confirms the success of sample preparation using the laser ablation technique, as the crystallite size range is nano-sized, which is very suitable for medical purposes, especially as a microbiological inhibitor. The XRD also showed that the sample was free of impurities, through the clear peaks related to nano-silver and the absence of other peaks that could indicate the presence of impurities. This supports the use of high-quality raw materials.

The XRD analysis noted that the Ag nanoparticles synthesized using PLAL show excellent crystalline quality compared to materials prepared by conventional techniques. This is due to the small particle size, significantly reduced microstrain (ϵ) and dislocation density of these samples, which leads to clear crystal stability, therefore, it is suitable for medical applications that require high performance.

Figure (5) shows the XRD pattern of the prepared silver nanoparticles. The average crystallite size, calculated using the Scherrer's equation, ranged from 20 to 32 nm, indicating the formation of stable, fine crystalline structures. Furthermore, the dislocation density was very low, indicating few structural defects and a high resistance to internal deformation. Microstrain (ϵ) values calculated using XRD data test and a clear relationship was found with the diffraction angle (2θ). When the angles were high, such as $2\theta = 78^\circ$, the micro strain was high (4.53×10^4), indicating increased distortion in the crystal lattice. Conversely, when the angles were low, such as $2\theta=39^\circ$, the microstrain (ϵ) was low (1.42×10^4), indicating reduced crystal distortion. These results indicate that strain increases with increasing FWHM and higher diffraction angles, which confirms this connection, but the final result is that the value of the very small strain is what enhances the small crystallite size of the sample and its good properties, which make it suitable for applications, especially medical ones.

The microstrain value was determined by using the Williamson-Hall method, which confirmed the crystal size calculations from the Scherrer's equation. The small crystal sizes, low microscopic strain, and low dislocation density obtained support the hypothesis that the particles produced using this technique exhibit distinct structural and mechanical properties, making them suitable for biomedical applications, particularly as antimicrobial inhibitors. This was confirmed by testing against two types of bacteria, which yielded very good results. The study of mechanical properties is of great importance in this context and is not limited to studying the structural properties of the material only, as it has been observed that enhancing the mechanical properties improves the interaction of the

nanomaterial with the cell membranes of microorganisms and thus increases its effectiveness as an antibiotic against these organisms.

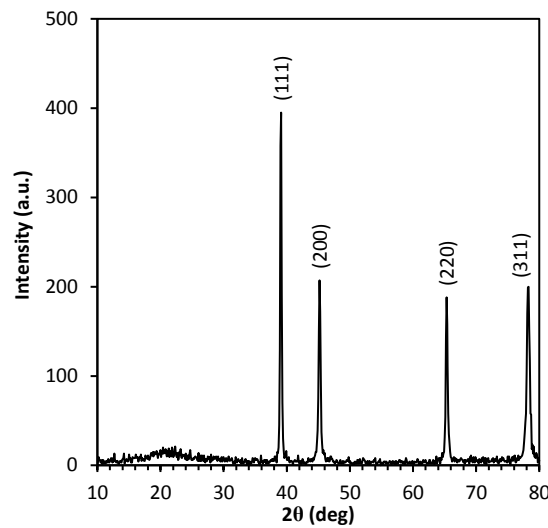


Fig. (5) XRD pattern of Ag nanoparticles

The sample (nanofilm) was examined using a field-emission scanning electron microscope (FE-SEM), which revealed that the particle size ranged in the nanometer range and that it was spherical in shape. These properties give nanofilm its ability to interact with other materials, enhancing its use in numerous medical and engineering applications. Spherical nanoparticles have a larger surface area than their natural counterparts, increasing their interaction with cells or tissues in biological applications.

Ag nanoparticles is a promising material that is applied in medicine, particularly in disease treatment and sterilization. The particles are characterized by Penetrating the cell wall of the microorganism, thus being employed to develop anti-microorganisms' drugs. In addition, their electrical and thermal properties can be exploited in other applications such as drug delivery systems and radiotherapy. Ag nanoparticles is a smart material whose properties can be modified to suit different requirements, such as changing the particle size or adding other materials to increase its effectiveness. The spherical shape of the particles makes them more efficient in targeted drug delivery systems because they diffuse easily and evenly throughout the body.

Based on the results shown in Fig. (6), these unique properties of nanosilver can be leveraged to develop more efficient and safer advanced medical devices in the future to improve medical and preventive care. The particle size distribution of the nanosilver sample showed that most particles were in the less than 50 nm range, as shown in Fig. (6c), indicating that the material has a fine size distribution that allows for increased surface area.

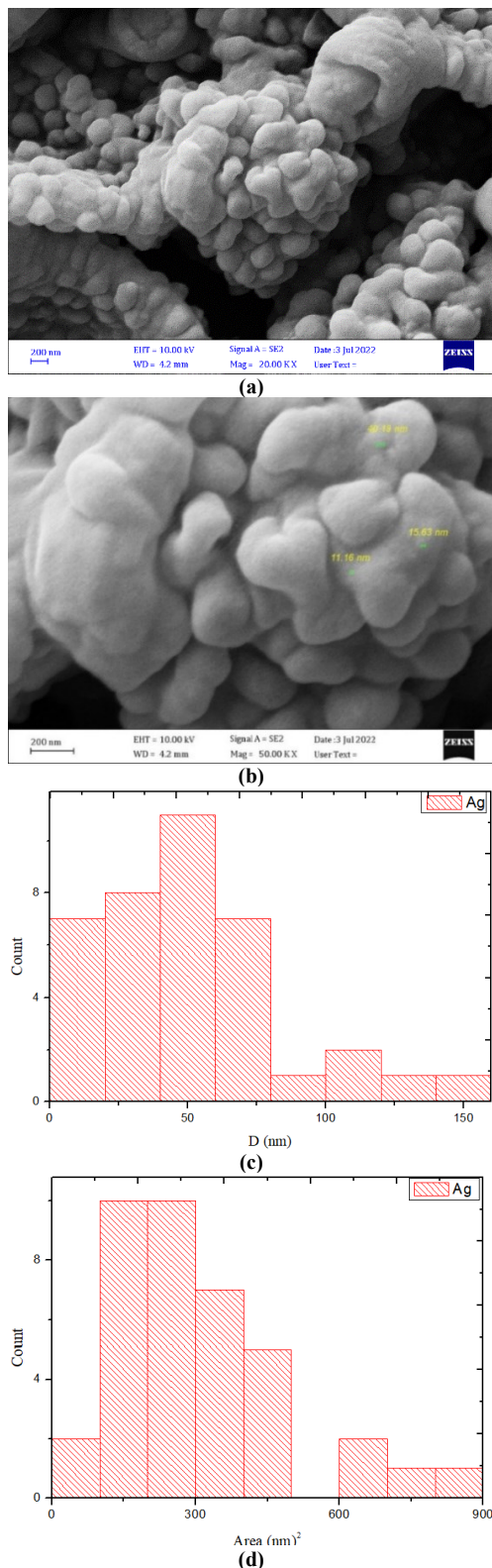


Fig. (6) (a) and (b) FE-SEM images of Ag nanoparticles, (c) Nanoparticle size distribution, (d) Nanoparticle area distribution

Additionally, the results showed that the surface area distribution of the particles was approximately $300 \text{ m}^2/\text{g}$ or less, as shown in Fig. (6d), enhancing the chemical with other material and biological with cell

wall of microorganisms reactivity of the nanoparticles. This distribution contributes to the improved properties of Ag nanoparticles, such as antibacterial activity, and increases its ability to interact with cells or tissues in medical applications. The large surface area enhances the particles' ability to interact with drugs or other compounds, thus forming effective vehicles for delivering drugs or therapeutic agents. Furthermore, the homogeneous distribution of the nanoparticles stabilizes the material and provides control over properties depending on the needs of diverse engineering or medical applications.

An antibacterial test was performed on Ag nanoparticles prepared using pulsed ablation technique to evaluate their performance against two types of bacteria: *Escherichia coli* (Gram-negative) and *Staphylococcus aureus* (Gram-positive) comparison between the effect of these particles on these two types of bacteria. The test indicated clear efficacy in inhibiting bacterial growth. A difference in growth inhibition was also observed between the two species, with *E. coli* measuring approximately 20-21 mm in diameter at concentrations of 100 and 200 $\mu\text{g}/\text{mL}$, respectively, while *Staphylococcus aureus* measured approximately 16 and 17 mm at the same concentrations (figures 7a and 7b). These results confirm that Ag nanoparticles have clear and promising antimicrobial effects, especially against bacteria in general and Gram-negative bacteria in particular.

Despite the widely documented high antibiotic resistance of this category of bacteria, since the construction of these bacteria's outer membrane is complex, the silver nanoparticles penetrated well through the cell wall and interacted with cellular elements, including proteins and enzymes, thereby effectively suppressing bacterial growth. Antibacterial activity of Ag nanoparticles is attributed to two mechanisms: interaction with the bacterial cell membrane, production of reactive oxygen species (ROS), and release of silver ions (Ag^+). The released silver ions further react with thiol groups of vital enzymes and DNA, ultimately leading to death of the bacterial cell. The results foretell the possibility of silver nanoparticles as an antibacterial compound, especially in use in wound dressings, sterilization coatings, and medical devices.

The antibacterial effect of silver nanoparticles can be enhanced by reducing particle size, surface charge, or improving mechanical properties at the microscopic level, or by combining them with other molecules to increase their biological activity. These findings justify the use of silver nanoparticles in biomedical applications to treat bacterial infections.

All images and graphs used in this research, particularly the structural and morphological investigations, have been reproduced in high resolution to ensure high clarity and are suitable for printing and publishing. Clear labels for the axes are also included,

along with the correct physical units, in a manner consistent with scientific presentation. Ensure that the data, graphs, and images represent the original results and are clearly presented and explained to the reader.

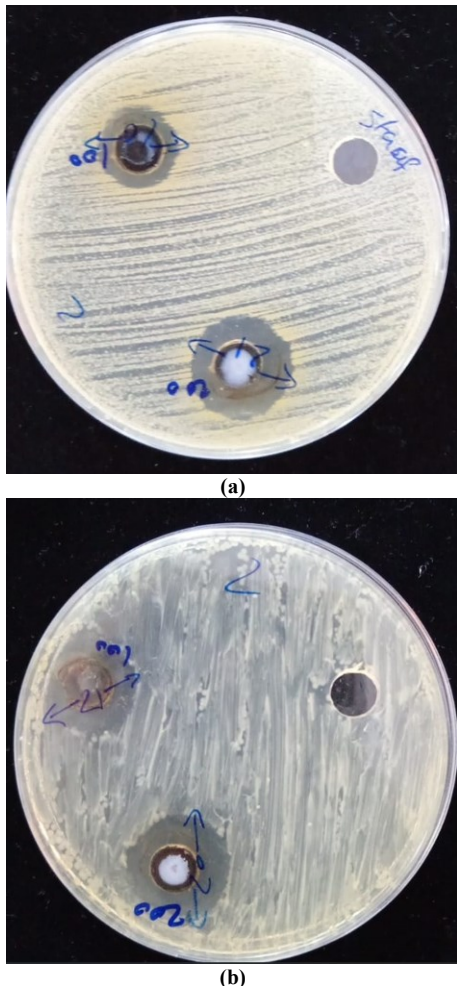


Fig. (7) Images of antimicrobial efficacy of Ag nanoparticles against (a) negative bacteria and (b) positive bacteria

4. Conclusion

Silver nanoparticles were successfully prepared in pure aqueous solution by pulsed laser ablation without the use of any chemicals. Analytical results indicated that the particles have distinct physical and chemical properties. An absorption peak was observed at ~ 425 nm, while surface bonds such as O-H and C-O were exhibited due to material-water and surroundings interaction, demonstrating stability. The optical energy gap of about 2.3 eV is likely resulting from surface plasmonic phenomena or inter-band transitions, given the absence of a conventional bandgap in pure silver. The crystalline nature of the particles was confirmed and the particles are spherical in shape with a diameter ranging from 10 to 50 nm. Biologically, the silver particles were very effective against Gram-negative and Gram-positive bacteria demonstrating their ability

to kill proteins and enzymes. The novelty of this work lies in utilizing a straightforward method to chemically clean small silver nanoparticles synthesized with pure, well-defined optical and crystalline properties and antibacterial activities, and enhancing their forthcoming applications in medicine and industry.

Acknowledgments

The author would like to express his sincere gratitude to the Nanotechnology and Advanced Materials Research Unit at the University of Kufa for providing technical support, laboratory facilities, and valuable guidance during the experimental work.

References

- [1] S. Malik, K. Muhammad and Y. Waheed, "Nanotechnology: A revolution in modern industry", *Molecules*, 28(2) (2023) 661.
- [2] B. Mekuye and B. Abera, "Nanomaterials: An overview of synthesis, classification, characterization, and applications", *Nano Select*, 4(8) (2023) 486-501.
- [3] Z. Hui et al., "Green flexible electronics: natural materials, fabrication, and applications", *Adv. Mater.*, 35(28) (2023) 2211202.
- [4] N. Mohammed et al., "Nanotechnology and its applications in industry and product design", *J. Textil. Color. Polym. Sci.*, 21(2) (2024) 273-284.
- [5] S. Tripathy, J. Rodrigues and N.G. Shimpi, "Top-down and Bottom-up Approaches for Synthesis of Nanoparticles", *Nanobiomater. Perspect. Med. Appl. Diagn. Treat. Dis.*, 145 (2023) 92-130.
- [6] S. Palagati and J. Reddy, "Synthesis by Top-Down and Bottom-Up", *Adv. Mater.: Product. Character. Multidiscip. Appl.*, (2024) 201.
- [7] A.H. Attallah et al., "Effect of liquid and laser parameters on fabrication of nanoparticles via pulsed laser ablation in liquid with their applications: a review", *Plasmonics*, 18(4) (2024) 1307-1323.
- [8] A.A. Manshina et al., "The second laser revolution in chemistry: emerging laser technologies for precise fabrication of multifunctional nanomaterials and nanostructures", *Adv. Func. Mater.*, 34(40) (2024) 2405457.
- [9] M. Alhajj and S.K. Ghoshal, "Sustainability, safety, biocompatibility and benefits of laser ablated gold, silver and copper nanoparticles: A comprehensive review", *J. Mol. Liquids*, 414A (2024) 126130.
- [10] I.Y. Khairani et al., "Green nanoparticle synthesis at scale: a perspective on overcoming the limits of pulsed laser ablation in liquids for high-throughput production", *Phys. Chem. Chem. Phys.*, 25(29) (2024) 19380-19408.
- [11] I. Karakaş, N. Hacıoğlu B.E. Özdemir, "Green Synthesis and Antibiofilm Activity of Silver Nanoparticles by *Camellia sinensis* L. (White Tea

Leaf)", *Kahramanmaraş Sütçü İmam Üniversitesi Tarım ve Doğa Dergisi*, 27(2) (2024) 285-292.

[12] P. Szczygiewska, A. Feliczkak-Guzik and I. Nowak, "Nanotechnology—general aspects: A chemical reduction approach to the synthesis of nanoparticles", *Molecules*, 28(13) (2023) 4932.

[13] Y. Ishikawa et al., "Pulsed laser melting in liquid for crystalline spherical submicrometer particle fabrication—Mechanism, process control, and applications", *Prog. Mater. Sci.*, 131 (2023) 101004.

[14] N.E.A. El-Naggar et al., "Myco-Biosynthesis of Silver Nanoparticles, Optimization, Characterization, and In Silico Anticancer Activities by Molecular Docking Approach against Hepatic and Breast Cancer", *Biomolecules*, 14(9) (2024) 1170.

[15] A. Luceri et al., "Silver nanoparticles: review of antiviral properties, mechanism of action and applications", *Microorgan.*, 11(3) (2023) 629.

[16] P.R. More et al., "Silver nanoparticles: bactericidal and mechanistic approach against drug resistant pathogens", *Microorgan.*, 11(2) (2023) 369.

[17] E. Hassan et al., "Preparation and characterization of ZnO nano-sheets prepared by different depositing methods", *Iraqi J. Sci.*, 63(2) (2022) 538-547.

[18] M. Al-saidi et al., "Extraction and characterization of nickel oxide nanoparticles from Hibiscus plant using green technology and study of its antibacterial activity", *Biomed.*, 42(6) (2022) 1290-1295.

[19] M.M. Dastani, M.H. AL-Ali and M. Moradi, "Influence of current annealing on the magneto-impedance response of co-based ribbons arising from surface structural improvement", *J. Non-Cryst. Solids*, 516 (2019) 9-13.

[20] M.H. Al-Saidi, and A.J. Ghazai, "Structural and mechanical properties of ZnO: MgO shape memory alloy for medical application", *J. Biosci. Appl. Res.*, 11(2) (2025) 549-564.

Table (1) XRD results of silver nanoparticles

2θ (deg)	FWHM (deg)	d (nm)	(hkl)	D (nm)	Dislocations x10 ⁴	Strain x10 ⁴
39.074	0.258	2.3034	111	32.67294	9.36750	1.42
45.209	0.342	2.004	200	25.16185	15.79483	2.73
65.321	0.353	1.4273	220	26.73182	13.99403	2.94
78.281	0.505	1.2203	311	20.28269	24.30797	4.53